



Numerical Computations of the PCD Method

Ahmed Tahiri

ABSTRACT: The PCD (piecewise constant distributions) method is a discretization technique of the boundary value problems in which the unknown distribution and its derivatives are represented by piecewise constant distributions but on distinct meshes. It has the advantage of producing the most sparse stiffness matrix resulting from the approximate problem. In this contribution, we propose a general triangulation with the PCD method by combining rectangular elements and triangular elements. We also apply this discretization technique for the 2D elasticity problem. We conclude by presenting the numerical results of the proposed method for the 2D diffusion equation.

Key Words: Boundary value problem, discretization technique, PCD method, compact schemes, most sparse stiffness matrix, elasticity problem, $O(h)$ -convergence rate.

Contents

1 Introduction	39
2 PCD discretization	40
2.1 Formulation of the problem	40
2.2 PCD spaces	40
2.3 General triangulation	44
2.4 PCD equations	44
2.5 Discrete Friedrichs inequalities	45
3 Convergence analysis	47
4 Application: Elasticity problem	49
5 Numerical experiments	50
6 Concluding remarks	53

1. Introduction

We present a discretization technique of boundary value problems (BVP) in which the unknown distribution as well as its derivatives are all represented by piecewise constant distributions, each one on a specific mesh. The interest for piecewise constant approximations has been highlighted since the early days of partial differential equations as a discretization techniques, being more or less explicitly

2010 *Mathematics Subject Classification:* 65N12, 65N15, 65N50.
 Submitted October 23, 2016. Published January 27, 2017

at the root of the control volume method widely used in engineering applications, particularly in computational fluid dynamics. This motivated the early analysis by [1], [2], [5] and [14] which raises its persistent interest as it is illustrated in many more recent works [4], [6], [7] and [8]. Our approach cannot however rely on the results obtained so far because we use piecewise constant approximations not only for the unknown distribution itself but also for its derivatives.

This feature requires the introduction of distinct meshes to represent each distribution and new mathematical tools for the convergence analysis of the resulting discrete schemes.

2. PCD discretization

2.1. Formulation of the problem

To keep the presentation of this discretization as simple as possible, we restrict the present contribution to the analysis of the 2D diffusion equation on a nonuniform rectangular mesh. The convergence analysis and the technical results of the PCD method can be found in [9] and [12]. The extension of the presented method on polygonal or L-shaped domain does not raise any difficulties.

We consider solving the following BVP on a rectangular domain Ω :

$$-\operatorname{div}(p(x)\nabla u(x)) + q(x)u(x) = s(x) \quad x \in \Omega \quad (2.1)$$

$$u(x) = 0 \quad x \in \Gamma_0 \quad (2.2)$$

$$n \cdot \nabla u(x) = 0 \quad x \in \Gamma_1 \quad (2.3)$$

where n denotes the unit normal to $\Gamma = \partial\Omega$ and $\Gamma = \Gamma_0 \cup \Gamma_1$. We assume that p and q are in $L^\infty(\Omega)$, that $p(x)$ is strictly positive on $\overline{\Omega}$, that $q(x)$ is nonnegative on Ω and that we have a well posed problem.

The discrete version of this problem will be based on its variational formulation:

$$\text{find } u \in H \text{ such that } \forall v \in H \quad a(u, v) = (s, v)_\Omega \quad (2.4)$$

where $H = H_{\Gamma_0}^1(\Omega) = \{v \in H^1(\Omega), v = 0 \text{ on } \Gamma_0\}$,

$$a(u, v) = \int_{\Omega} p(x) \nabla u(x) \cdot \nabla v(x) dx + \int_{\Omega} q(x)u(x)v(x) dx, \quad (2.5)$$

and $(s, v)_\Omega$ denotes the $L^2(\Omega)$ scalar product.

2.2. PCD spaces

The PCD discretization splits the open domain Ω under investigation into elements Ω_ℓ , $\ell \in J$, open subsets of Ω , such that

$$\overline{\Omega} = \bigcup_{\ell \in J} \overline{\Omega}_\ell \quad \Omega_k \cap \Omega_\ell = \emptyset \text{ if } k \neq \ell \quad \forall k, \ell \in J$$

and defines several sub-meshes on each element Ω_ℓ for the representation of $v \in H^1(\Omega)$ and of its derivatives $\partial_i v$ ($i = 1, 2$). These representations, denoted v_h and $\partial_{h_i} v_h$ ($i = 1, 2$) respectively, are piecewise constant on each of these sub-meshes (a specific one for each) with the additional requirement for v_h that it must be continuous across the element boundaries (i.e. along the normal to the element boundary).

Here, we consider rectangular meshes and the operators ∂_{h_i} ($i = 1, 2$) are finite difference quotients taken along the element edges.

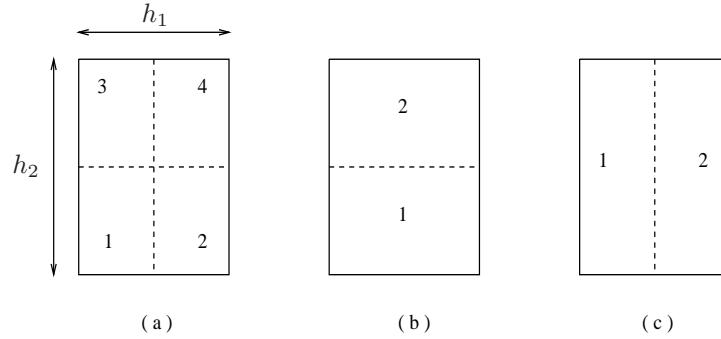


Figure 1: Sub-meshes used to represent v_h (a), $\partial_{h_1} v_h$ (b) and $\partial_{h_2} v_h$ (c) on Ω_ℓ

The sub-meshes used to define $v_h|_{\Omega_\ell}$, $\partial_{h_1} v_h|_{\Omega_\ell}$ and $\partial_{h_2} v_h|_{\Omega_\ell}$ on a rectangular element Ω_ℓ are represented on Fig. 1.

$v_h|_{\Omega_\ell}$ is the piecewise constant distribution with 4 values v_{hi} on the regions denoted i with $i = 1, \dots, 4$ on Fig. 1 (a).

$\partial_{h_1} v_h|_{\Omega_\ell}$ is the piecewise constant distribution with constant values:

$$(\partial_{h_1} v_h)_1 = \frac{v_{h2} - v_{h1}}{h_1}, \quad (\partial_{h_1} v_h)_2 = \frac{v_{h4} - v_{h3}}{h_1}$$

on the regions denoted 1, 2 on Fig. 1 (b).

Similarly, $\partial_{h_2} v_h|_{\Omega_\ell}$ is the piecewise constant distribution with constant values:

$$(\partial_{h_2} v_h)_1 = \frac{v_{h3} - v_{h1}}{h_2}, \quad (\partial_{h_2} v_h)_2 = \frac{v_{h4} - v_{h2}}{h_2}$$

on the regions denoted 1, 2 on Fig. 1 (c).

In addition, v_h must be continuous across element boundaries. Thus for example if the bottom boundary of Ω_ℓ is common with the top boundary of Ω_k , one must have that $v_{h1}(\Omega_\ell) = v_{h3}(\Omega_k)$ and $v_{h2}(\Omega_\ell) = v_{h4}(\Omega_k)$.

It is of interest to note that $\partial_{h_i} v_h$ has the following property:

$$\int_P^Q \partial_{h_i} v_h dx_i = v_h(Q) - v_h(P) \quad (2.6)$$

for any pair of nodes $\{P, Q\}$ of the mesh.

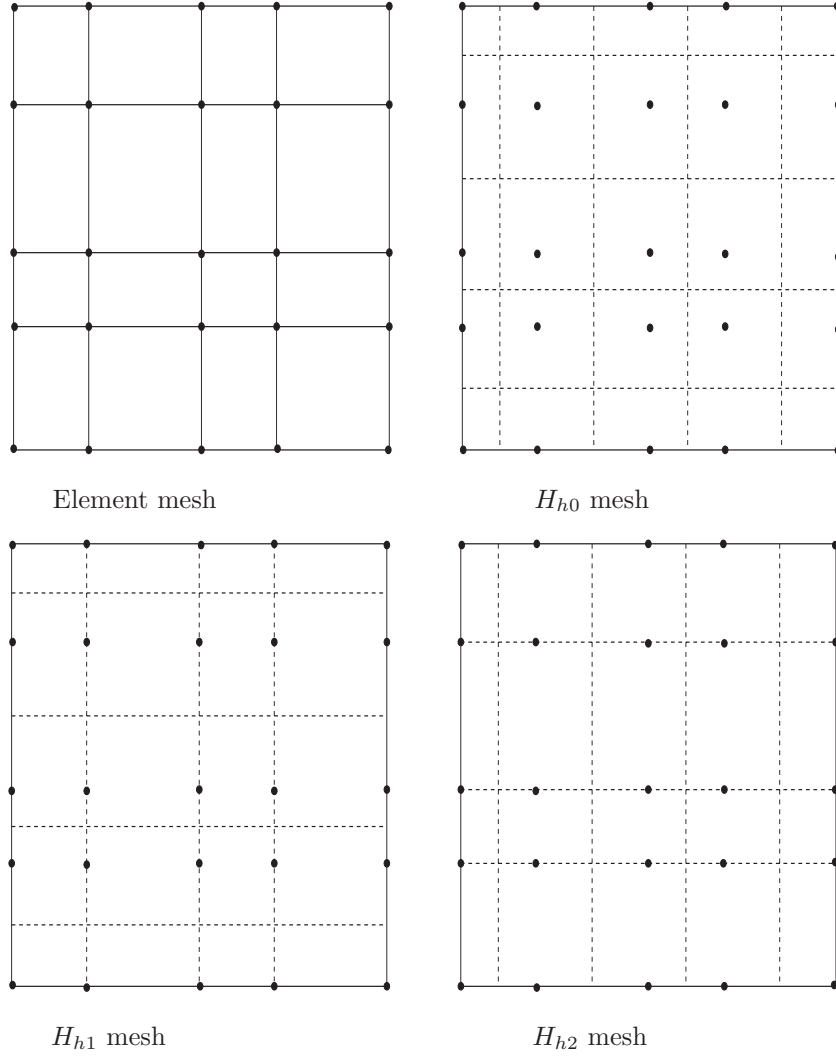


Figure 2: Discrete meshes

The spaces associated with this discretization are defined as follows. E denotes $(L^2(\Omega))^3$ with norm $\| (u, v, w) \|_E^2 = \| u \|^2 + \| v \|^2 + \| w \|^2$. F denotes the subspace of E of the elements of the form $(v, \partial_1 v, \partial_2 v)$.

H_{h0} and H_{hi} ($i = 1, 2$) denote the spaces of piecewise constant distributions used

to define v_h and $\partial_{hi} v_h$ ($i = 1, 2$), equipped with the $L^2(\Omega)$ scalar product. $E_h = H_{h0} \times H_{h1} \times H_{h2}$ with norm $\| (u_h, v_h, w_h) \|_E^2 = \| u_h \|^2 + \| v_h \|^2 + \| w_h \|^2$ and F_h is the subspace of E_h of the elements of the form $(v_h, \partial_{h1} v_h, \partial_{h2} v_h)$. We further denote by H_h the space H_{h0} equipped with the inner product:

$$(v_h, w_h)_h = (v_h, w_h)_\Omega + \sum_{i=1}^2 (\partial_{hi} v_h, \partial_{hi} w_h)_\Omega, \quad (2.7)$$

and its associate norm is denoted $\| \cdot \|_h$.

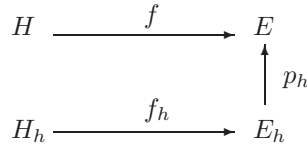
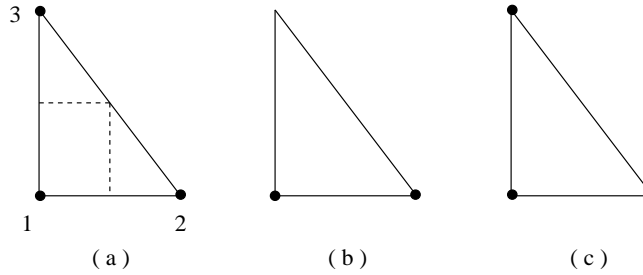


Figure 3: Structure of the discretization analysis

Clearly H and H_h are isomorphic to F and F_h respectively and we let f and f_h denote the bijections of H and H_h into E and E_h ($F = f(H)$ and $F_h = f_h(H_h)$). We further denote by p_h the canonical injection of E_h into E . These operators are represented on Fig. 3.

The motivation for using this space structure is that, while we cannot directly compare the elements of H and H_h , we can use the norm of E to measure the distance between elements $f(v) = (v, \partial_1 v, \partial_2 v)$ of F and $f_h(v_h) = (v_h, \partial_{h1} v_h, \partial_{h2} v_h)$ of F_h .

Figure 2 (top-left) provides an example of a rectangular element mesh. On the same figure we also represent the meshes H_{h0} and H_{hi} ($i = 1, 2$) used to define the piecewise constant distributions v_h and $\partial_{hi} v_h$, $i = 1, 2$. Each of these meshes defines cells which are useful for distinct purposes. The elements are denoted by Ω_ℓ , $\ell \in J$; we similarly denote the cells of the other meshes by $\Omega_{\ell i}$, $\ell \in J_i$, $i = 0, 1, 2$ respectively. It is of interest to note that each node of the element mesh may be uniquely associated with a cell of H_{h0} ; we therefore denote them by N_ℓ , $\ell \in J_0$. The mesh size, denoted h , is defined as: $h = \max(h_\ell)$, $\ell \in J$ with $h_\ell = \text{diam}(\Omega_\ell)$

Figure 4: Triangular element Ω_ℓ

2.3. General triangulation

We note that triangular elements may also be used in the PCD discretization. For this purpose we consider a rectangular triangular element Ω_ℓ and we define the sub-meshes, on such element, used to define the representations v_h , $\partial_{h1} v_h$, and ∂_{h2} .

In this case $v_h|_{\Omega_\ell}$ assumes 3 values (Fig. 4 (a)), the representation $\partial_{h1} v_h$ assumes 1 value (Fig. 4 (b))

$$(\partial_{h1} v_h)_{\Omega_\ell} = \frac{v_{h2} - v_{h1}}{h_{12}}$$

and the representation $\partial_{h2} v_h$ assumes 1 value (Fig. 4 (c))

$$(\partial_{h2} v_h)_{\Omega_\ell} = \frac{v_{h3} - v_{h1}}{h_{13}}$$

where h_{ij} is the distance between the nodes N_i and N_j ($1 \leq i, j \leq 3$). Also here we require the continuity of v_h across the element boundaries.

In this way, the method can accommodate any shape of polygonal domains through the combined use of rectangular elements and triangular elements.

We note that the use of rectangular and triangular elements is not a restriction of the PCD discretization. Other elements and other forms of sub-meshes on such elements can be used, see [3]. We note that the property (2.6) is still valid even if we have combine the rectangular elements and the rectangular triangular elements. Also this property is still valid even if we introduce a local mesh refinement, see [9], [10] and [12].

2.4. PCD equations

We now define the discrete problem to be solved in H_h by

$$\text{find } u_h \in H_h \text{ such that } \forall v_h \in H_h \quad a_h(u_h, v_h) = (s, v_h)_\Omega \quad (2.8)$$

$$\text{where } a_h(u_h, v_h) = \sum_{i=1}^2 (p(x) \partial_{hi} u_h, \partial_{hi} v_h)_\Omega + (q(x) u_h, v_h)_\Omega \quad (2.9)$$

The discrete matrix is obtained as usual by introducing a basis $(\phi_i)_{i \in J_0}$ of the space H_h , expanding the unknown u_h in this basis $u_h = \sum_{i \in J_0} \xi_i \phi_i$ and expressing the variational condition (2.8) by

$$a_h(u_h, \phi_j) = \sum_{i \in J_0} a_h(\phi_j, \phi_i) \xi_i = (s, \phi_j)_\Omega \text{ for all } j \in J_0$$

Whence, the linear system $\mathcal{A} \xi = b$ with stiffness matrix $\mathcal{A} = (a_{ij}) = (a_h(\phi_i, \phi_j))$, right hand side b with components $b_j = (s, \phi_j)_\Omega$, $j \in J_0$ and unknown vector ξ with components ξ_i , $i \in J_0$.

It should be stated that the presented method has the advantage of producing the most compact schemes. Also, it leads to the most sparse stiffness matrix resulting from the approximate problem.

2.5. Discrete Friedrichs inequalities

Here we present the following lemmas that represent a discrete version of first and second Friedrichs inequalities and trace inequality for the proposed discretization.

Lemma 2.1. *Let Ω be a connected bounded polygonal domain. We assume that $\Gamma_0 = \partial\Omega$. Then, there exists a constant $C > 0$, independent of h such that:*

$$\|v_h\|^2 \leq C (\|\partial_{h1} v_h\|^2 + \|\partial_{h2} v_h\|^2) \quad \forall v_h \in H_h \quad (2.10)$$

Proof: This lemma is a discrete version of the first *Friedrichs* inequality. We give its proof on a square $(0, a) \times (0, a)$ since we can include all connected bounded polygonal domain in a square.

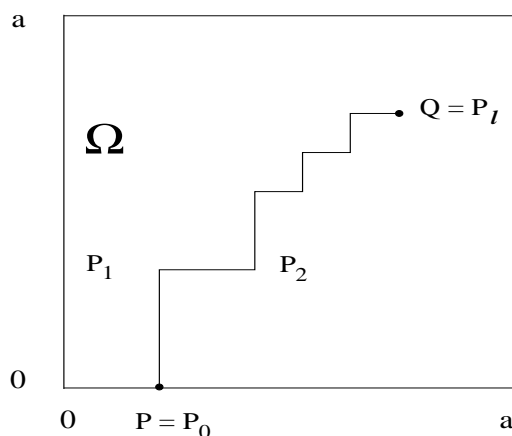


Figure 5: Example of path

Let the bounded open square $(0, a) \times (0, a)$ with sides parallel to the axes x_1 and x_2 .

Letting P and Q be two nodes such that $P \in \partial\Omega$ and $Q \in \Omega \subset (0, a) \times (0, a)$, there is a path of the form $S = \{P_0, P_1, P_2, \dots, P_l\}$ connecting $P_0 = P$ and $P_l = Q$ (made up of a succession of mesh grid segments, see Fig. 5) such that

$$v_h(Q) = \int_S \partial_{hi} v_h dx_i$$

where $i = 1$ on horizontal segments and $i = 2$ on vertical segments. Subdividing S into $S = S_1 \cup S_2$ where S_1 is the union of horizontal segments and S_2 the union of vertical segments, one may write

$$v_h(Q) = \int_{S_1} \partial_{h1} v_h dx_1 + \int_{S_2} \partial_{h2} v_h dx_2$$

whence,

$$|v_h(Q)| \leq \left(\int_{S_1} dx_1 \right)^{\frac{1}{2}} \left(\int_{S_1} |\partial_{h1} v_h|^2 dx_1 \right)^{\frac{1}{2}} + \left(\int_{S_2} dx_2 \right)^{\frac{1}{2}} \left(\int_{S_2} |\partial_{h2} v_h|^2 dx_2 \right)^{\frac{1}{2}}$$

Then,

$$|v_h(Q)| \leq a^{1/2} \left(\int_{S_1} |\partial_{h1} v_h|^2 dx_1 \right)^{1/2} + a^{1/2} \left(\int_{S_2} |\partial_{h2} v_h|^2 dx_2 \right)^{1/2}$$

Therefore (by $(\alpha + \beta)^2 \leq 2\alpha^2 + 2\beta^2$)

$$|v_h(Q)|^2 \leq 2a \left(\int_{S_1} |\partial_{h1} v_h|^2 dx_1 \right) + 2a \left(\int_{S_2} |\partial_{h2} v_h|^2 dx_2 \right)$$

Integrating this inequality on the domain Ω

$$\|v_h\|^2 \leq 2a^2 (\|\partial_{h1} v_h\|^2 + \|\partial_{h2} v_h\|^2)$$

which is the inequality (2.10) with $C = 2a^2$. \square

This Lemma and this proof are still valid if Γ_0 has a positive measure and $\Gamma_0 \neq \partial\Omega$. In such case, we can choose the node P such that $P \in \Gamma_0$ and we prove (2.10) by the same argument.

In similar way, we can prove the following lemmas which give a *discrete Friedrichs second inequality* and a *discrete trace inequality* for the proposed discretization in the case where Γ_0 has a positive measure, see [9].

Lemma 2.2. *Let Ω be a connected bounded polygonal domain. Then, there exists a constant $C > 0$, independent of h such that:*

$$\|v_h\|_h \leq C (\|\partial_{h1} v_h\|^2 + \|\partial_{h2} v_h\|^2 + \|v_h\|_\Gamma^2)^{1/2} \quad \forall v_h \in H_h \quad (2.11)$$

Lemma 2.3. *Let Ω be a connected bounded polygonal domain. Then, there exists a constant $C > 0$, independent of h such that:*

$$\int_{\Gamma} v_h(x)^2 ds = \|v_h\|_{\Gamma}^2 \leq C \|v_h\|_h^2 \quad \forall v_h \in H_h \quad (2.12)$$

Using these lemmas we can prove that $a_h(u_h, v_h)$ is uniformly coercive on H_h . Therefore, the associated norm

$$\|v_h\|_{a_h} = (a_h(v_h, v_h))^{1/2}$$

is uniformly equivalent to the norm of H_h , i.e. there exists positive constants α, β independent of the mesh size h such that:

$$\forall v_h \in H_h \quad \alpha \|v_h\|_h \leq \|v_h\|_{a_h} \leq \beta \|v_h\|_h .$$

On the other hand, since $p(x)$ and $q(x)$ are in $L^\infty(\Omega)$, it is clear that $a_h(u_h, v_h)$ is uniformly continuous on H_h . Therefore, the problem (2.8) has a unique solution.

3. Convergence analysis

As mentioned in Sect. 2, the error between the solution $u \in H$ of (2.1) and the discrete solution $u_h \in H_h$ of (2.8) will be measured by the distance between their representations in E , namely

$$\|f(u) - f_h(u_h)\|_E \quad (3.1)$$

As usual, the bounds that can be obtained depend on the regularity of u . Here, we assume that $u \in H^2(\Omega)$. In that case, u is continuous on $\overline{\Omega}$ and we can then define its interpolant u_I in H_h through

$$u_I(N_\ell) = u(N_\ell) \text{ for all nodes } N_\ell, \ell \in J_0 \quad (3.2)$$

and rely on interpolation theory in H_h .

More specifically, we can then use the following result proved in [9], [10] and [12].

Lemma 3.1. *Under the general assumptions and notation defined above, there exists a positive constant C independent of the mesh size h such that*

$$\forall v \in H^2(\Omega) \quad \|f(v) - f_h(v_I)\|_E \leq C h \|v\|_{2,\Omega} \quad (3.3)$$

where v_I denotes the interpolant of v in H_h .

By this result, it remains to bound the error between u_I and the approximate solution u_h : $\|f_h(u_I) - f_h(u_h)\|_E = \|u_I - u_h\|_h$.

Since the a_h -norm is uniformly equivalent to the H_h -norm, we may equivalently try to bound $\|u_I - u_h\|_{a_h}$ defined by

$$\|u_I - u_h\|_{a_h} := \sup_{\substack{v_h \in H_h \\ v_h \neq 0}} \frac{|a_h(u_I, v_h) - a_h(u_h, v_h)|}{\|v_h\|_h} \quad (3.4)$$

$$= \sup_{\substack{v_h \in H_h \\ v_h \neq 0}} \frac{|a_h(u_I, v_h) - a(u, v_h)|}{\|v_h\|_h}$$

because, $\forall v_h \in H_h$ $a_h(u_h, v_h) = (s, v_h)_\Omega = a(u, v_h)$

Since $s(x)$ is still defined on H_h and $s(x)$ is replaced by its value in (2.1). In the term $a(u, v_h)$, the derivatives of v_h are understood in distributions sense. By introducing some restrictions the expression $a(u, v_h)$ can be defined.

More explicitly:

$$\begin{aligned} a_h(u_I, v_h) - a(u, v_h) &= (p(x) \partial_{h1} u_I, \partial_{h1} v_h)_\Omega + (p(x) \partial_{h2} u_I, \partial_{h2} v_h)_\Omega \\ &- (p(x) \partial_1 u, \partial_1 v_h)_\Omega - (p(x) \partial_2 u, \partial_2 v_h)_\Omega + (q(x)(u_I - u), v_h)_\Omega \end{aligned} \quad (3.5)$$

To bound (3.5), we may try to bound separately the terms:

$(q(x)(u_I - u), v_h)_\Omega$ and $(p(x) \partial_{hi} u_I, \partial_{hi} v_h)_\Omega - (p(x) \partial_i u, \partial_i v_h)_\Omega$, ($i = 1, 2$).

The first term is bounded by using Lemma (3.1). The last terms are most easily analyzed and bounded on the cells $\Omega_{\ell i}$ of the H_{hi} meshes ($i = 1, 2$). Being similar in both cases, we consider $i = 1$, the contribution of an arbitrary cell $\Omega_{\ell 1}$ is:

$$\begin{aligned} A_1^\ell &= (p(x) \partial_{h1} u_I, \partial_{h1} v_h)_{\Omega_{\ell 1}} - (p(x) \partial_1 u, \partial_1 v_h)_{\Omega_{\ell 1}} \\ &= (p(x) \partial_{h1} u_I, \partial_{h1} v_h)_{\Omega_{\ell 1}} - \int_{E_\ell} p(x) \partial_1 u (v_2 - v_1) ds \end{aligned}$$

where $(v_2 - v_1)$ is the jump of v_h through the vertical median line E_ℓ of the cell $\Omega_{\ell 1}$.

It should be noticed that $\partial_1 v_h$ (respectively $\partial_2 v_h$) is reduced to Dirac distributions taken along the edges of the regions where v_h is constant weighted by the corresponding discontinuity of v_h , the vertical median line of the cell $\Omega_{\ell 1}$ of the H_{h1} meshes in this case (respectively the horizontal median line of the cell $\Omega_{\ell 2}$ of the H_{h2} meshes).

However, in the expression of the error, we now see that $\partial_1 v_h$ and $\partial_2 v_h$ appear with Dirac behaviors across these lines. This is clearly incompatible with the coefficient $p(x)$ that would be discontinuous across the same lines.

To avoid such situations, we must introduce restrictions on the choice of the mesh, namely that material discontinuities (i. e. discontinuities of $p(x)$) should never match grid lines of the H_{h0} mesh. The best practical way to ensure this restriction is to require that material discontinuities be always grid lines of the element mesh. By introducing this restriction the expression $a(u, v_h)$ is well defined.

Under the mentioned restrictions and the regularity of u the exact solution of (2.1), we can give the following Theorem, for the proof see [9] and [12].

Theorem 3.2. *Assume that the solution u of (2.1) belongs to $H^2(\Omega)$. Then, there exists a constant $C > 0$ (independent of h), such that:*

$$\|u_I - u_h\|_h = \|f_h(u_I) - f_h(u_h)\|_E \leq Ch \|u\|_{2,\Omega}$$

and

$$\|f(u) - f_h(u_h)\|_E \leq Ch \|u\|_{2,\Omega}$$

where u_h is the solution of the problem (2.8).

The result of the previous theorem is still valid if the solution of the problem (2.8) is only locally H^2 -regular. Under higher regularity assumptions an error bound of order $O(h^2)$ can be obtained. If the solution u is only in $H^1(\Omega)$, we can still prove the convergence of u_h to u , see [9] and [12].

4. Application: Elasticity problem

We consider the boundary value problem: find $\mathbf{u} = (u_1, u_2)$ in $(H^1(\Omega))^2$ which satisfies the following equation in the domain Ω .

$$-\mu \Delta \mathbf{u}(x) - (\lambda + \mu) \operatorname{grad}(\operatorname{div} \mathbf{u}(x)) = \mathbf{s}(x) \text{ in } \Omega \quad (4.1)$$

$$\mathbf{u}(x) = 0 \text{ on } \Gamma_0 \quad (4.2)$$

$$n \cdot \nabla \mathbf{u}(x) = 0 \text{ on } \Gamma_1 \quad (4.3)$$

where n denotes the unit normal to $\Gamma = \partial\Omega$ and $\Gamma = \Gamma_0 \cup \Gamma_1$. We assume that μ and λ are two constants such that $\mu \geq \mu_0 > 0$, $\lambda > 0$, $\mathbf{s} = (s_1, s_2)$ in $(L^2(\Omega))^2$.

We assume that this problem is well posed and has a unique solution in $\mathbf{H} = (H_{\Gamma_0}^1(\Omega))^2$ equipped with the product norm:

$$\forall \mathbf{v} = (v_1, v_2) \in \mathbf{H}, \|\mathbf{v}\|_1^2 = \|v_1\|_1^2 + \|v_2\|_1^2$$

The variational formulation of this problem can be written:

$$\text{find } \mathbf{u} \in \mathbf{H} \text{ such that } \forall \mathbf{v} \in \mathbf{H}: \mathbf{a}(\mathbf{u}, \mathbf{v}) = \mathbf{s}(\mathbf{v}) \quad (4.4)$$

where

$$\mathbf{a}(\mathbf{u}, \mathbf{v}) = \int_{\Omega} [\lambda \operatorname{div} \mathbf{u}(x) \operatorname{div} \mathbf{v}(x) + 2\mu \sum_{i,j=1}^2 \epsilon_{i,j}(\mathbf{u})(x) \epsilon_{i,j}(\mathbf{v})(x)] dx \quad (4.5)$$

$$\mathbf{s}(\mathbf{v}) = \int_{\Omega} \mathbf{s}(x) \mathbf{v}(x) dx = \sum_{i=1}^2 \int_{\Omega} s_i(x) v_i(x) dx \quad (4.6)$$

$$\epsilon_{i,j}(\mathbf{u}) = \frac{1}{2} \left(\frac{\partial u_i}{\partial x_j} + \frac{\partial u_j}{\partial x_i} \right), \quad 1 \leq i, j \leq 2$$

Also here we use the same discretization technique to define an approximate problem of (4.4). The space H_{h0} is used to define the representation for each component v_i ($i = 1, 2$) of \mathbf{v} . The space H_{h1} (respectively H_{h2}) is used to define the representation for the partial derivatives components $\partial_1 v_i$ ($i = 1, 2$) (respectively $\partial_2 v_i$ ($i = 1, 2$)).

For this application (elasticity problem), the discrete space \mathbf{H}_h is the space $H_{h0} \times H_{h0}$ equipped with the norm:

$$\forall \mathbf{v}_h = (v_h^1, v_h^2) \in \mathbf{H}_h, \quad \|\mathbf{v}_h\|_h^2 = \|v_h^1\|_h^2 + \|v_h^2\|_h^2$$

We now define the approximate problem to be solved in \mathbf{H}_h by:

$$\text{find } \mathbf{u}_h \in \mathbf{H}_h \text{ such that } \forall \mathbf{v}_h \in \mathbf{H}_h : \mathbf{a}_h(\mathbf{u}_h, \mathbf{v}_h) = \mathbf{s}(\mathbf{v}_h) \quad (4.7)$$

where

$$\begin{aligned} \mathbf{a}_h(\mathbf{u}_h, \mathbf{v}_h) &= \int_{\Omega} \lambda \left(\sum_{i=1}^2 \partial_{hi} u_h^i \right) \left(\sum_{i=1}^2 \partial_{hi} v_h^i \right) dx \\ &+ 2\mu \int_{\Omega} \left(\sum_{i,j=1}^2 \epsilon_{i,j}^h(\mathbf{u}_h)(x) \epsilon_{i,j}^h(\mathbf{v}_h)(x) \right) dx \end{aligned} \quad (4.8)$$

$$\epsilon_{i,j}^h(\mathbf{u}_h) = \frac{1}{2} \left(\partial_{hj} u_h^i + \partial_{hi} u_h^j \right), \quad 1 \leq i, j \leq 2,$$

and $\mathbf{s}(\mathbf{v}_h)$ is still defined by (4.6).

Also here this discretization technique leads to the most sparse stiffness matrix from the approximate problem (4.7).

By the same analysis as in the previous section, we can bound the error between $\mathbf{u} = (u_1, u_2)$ the exact solution of (4.4) and $\mathbf{u}_h = (u_h^1, u_h^2)$ the exact solution of (4.7). Then, we can write the following error estimate:

$$\|f(u_1) - f_h(u_h^1)\|_E \leq C h \|u_1\|_2 \text{ and } \|f(u_2) - f_h(u_h^2)\|_E \leq C h \|u_2\|_2$$

5. Numerical experiments

In this section we present experimental results concerning the PCD discretization. We consider the domain Ω as the unit square $]0, 1[\times]0, 1[$. We denote by \mathcal{A} the stiffness matrix arising from the approximate problem (2.8), u_h denotes its solution and N denotes the number of unknowns. u is the exact solution of (2.1) and u_I its interpolant in H_h . We consider the following error estimators: the relative L^2 -error ε_0^r and the relative H^1 -error ε_1^r , defined by:

$$\varepsilon_0^r = \frac{\|u - u_h\|_0}{\|u\|_0}; \quad \varepsilon_1^r = \frac{|(u_I - u_h)^t \mathcal{A} (u_I - u_h)|^{1/2}}{\|u_I\|_h} = \frac{\|u_I - u_h\|_h}{\|u_I\|_h}$$

We consider the problem:

$$-\operatorname{div}(\nabla u(x, y)) = s(x, y) \text{ in } \Omega \text{ and } u(x, y) = 0 \text{ on } \partial\Omega .$$

We consider 3 examples, in the first one (respectively the second) we choose the source term $s(x, y)$ such that the exact solution is $u_1(x, y) = x(x - 1)y(y - 1)$ (respectively $u_2(x, y)$), the results of this example are presented in Table 1 (respectively Table 2), where

$$u_2(x, y) = \left(\frac{1}{1 + (2x - 1)^2} - \frac{1}{2} \right) \left(\frac{1}{1 + (2y - 1)^2} - \frac{1}{2} \right)$$

In Table 3 we present the results of the third example where the exact solution is: $u_3(x, y) = x(1 - x)y(1 - y)\beta(x, y)$, where $\beta(x, y) = \exp(-100 \{ (x - 0.5)^2 + (y - 0.5)^2 \})$. This solution has a sharp peak in the point $(0.5, 0.5)$ and varies much more rapidly in $\Omega_1 = [1/4, 3/4] \times [1/4, 3/4]$ than the remaining part of Ω .

h^{-1}	N	ε_0^r	ε_1^r
8	49	1.908×10^{-2}	1.931×10^{-2}
16	225	4.819×10^{-3}	4.891×10^{-3}
32	961	1.207×10^{-3}	1.226×10^{-3}
64	3969	3.021×10^{-4}	3.069×10^{-4}
128	16129	7.554×10^{-5}	7.674×10^{-5}
256	65025	1.888×10^{-5}	1.918×10^{-5}

Table 1: Results of the first example

h^{-1}	N	ε_0^r	ε_1^r
8	49	3.066×10^{-2}	3.471×10^{-2}
16	225	7.624×10^{-3}	8.646×10^{-3}
32	961	1.903×10^{-3}	2.159×10^{-3}
64	3969	4.756×10^{-4}	5.397×10^{-4}
128	16129	1.197×10^{-4}	1.249×10^{-4}
256	65025	2.972×10^{-5}	3.143×10^{-5}

Table 2: Results of the second example

h^{-1}	N	ε_0^r	ε_1^r
8	49	1.005	0.9599
16	225	0.4231	0.5668
32	961	0.2219	0.3094
64	3969	0.1122	0.1582
128	16129	5.631×10^{-2}	7.954×10^{-2}
256	65025	2.817×10^{-2}	3.982×10^{-2}

Table 3: Results of the third example

From Tables 1–3 we observe a monotonic improvement of the accuracy in both error estimators ε_0^r and ε_1^r , they decrease when N increases.

From Table 1–2, we observe that ε_0^r and ε_1^r are reduced by a factor of 4 when the mesh size is reduced by a factor of 2. Then, we have an $O(h^2)$ convergence rate, for the both norms, since we have a very smooth solutions. That proves, under higher regularity assumption, the presented method has the standard $O(h^2)$ convergence rate.

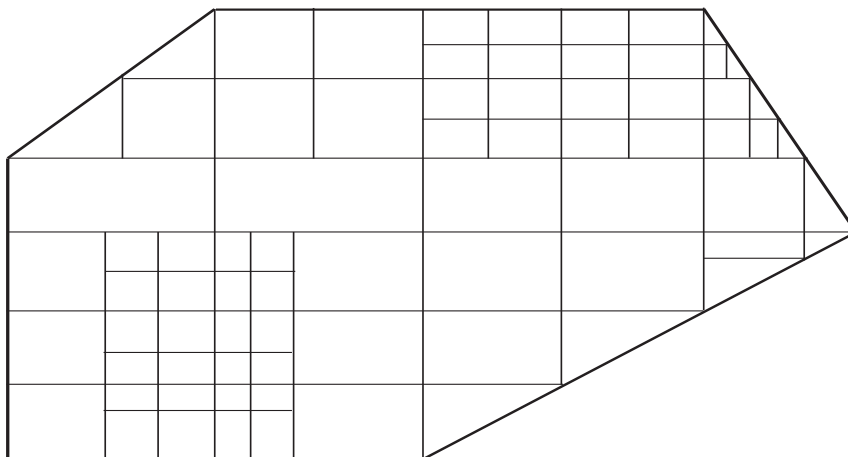
In the third example (Table 3), We observe that ε_0^r and ε_1^r are reduced by a factor of 2 when the mesh size is reduced by a factor of 2. Since the solution $u_3(x, y)$ has a sharp peak and an important variation in Ω_1 than the remaining part of Ω , the presented method has only an $O(h)$ convergence rate.

For the three examples, our numerical results are in agreement with the theoretical results given in Sect. 3.

We can improve the numerical results for the example 3 by introducing a local mesh refinement without slave nodes which does not raise new complexity, see [9], [11] and [12]. Furthermore, the PCD method can accommodate any shape of the domain by using triangular elements and still produces a reduced size of the approximate problem.

More explicitly, in Table 3 we must have an uniform mesh with 65025 nodes to get $\varepsilon_0^r = 2.817 \times 10^{-2}$ and the local L^2 -error around the point (0.5, 0.5) is 3.092×10^{-2} . With a local mesh refinement we get for $\varepsilon_0^r = 2.434 \times 10^{-2}$ only with the use of 28545 nodes and the local L^2 -error around the point (0.5, 0.5) is 7.547×10^{-4} . For more numerical tests and for the best local refinement strategy, we refer to [9], [11] and [13].

We illustrate on Fig. 6 an example of general triangulation of a polygonal domain Ω by combining rectangular elements, triangular elements and local mesh refinement.

Figure 6: General triangulation of the domain Ω

6. Concluding remarks

The main issue of the present work is the presentation of a BVP discretization method on polygonal domain. It is based on the use of piecewise constant distributions to represent the unknown distribution as well as its derivatives on distinct meshes. The PCD method has the advantage of producing the most sparse stiffness matrix resulting from the approximate problem, and has the standard first order estimate under the H^2 -regularity of the exact solution. The method is presented in the case of the diffusion equation but it can be applied in the other cases (elasticity problem for example), see [9] and [10]. We note that, with the PCD method we can introduce a local mesh refinement without slave nodes and it is still producing the most sparse stiffness matrix, see [9], [11], [12] and [13]. This local refinement improves the accuracy of the approximate solution without additional difficulties. Also, we note that we can combine the use of local mesh refinement and triangular elements in order to be able to follow any shape on the domain Ω and to reduce the size of the approximate problem.

References

1. J. P. Aubin, Approximation des espaces de distributions et ses opérateurs différentiels, Bull. Soc. Math. France, 12 (1967), 1-139.
2. R. E. Bank and D. J. Rose, Some error estimates for the box method, SIAM J. Num. Anal. 24 (1987), 777-787.
3. R. Beauwens, Forgivable variational crimes, Lecture Notes in Computer Science, 2542 (2003), 3-11.
4. Z. Cai, J. Mandel and S. McCormick, The finite volume element method for diffusion equations on general triangulations, SIAM J. Numer. Anal. 28 (1991), 392-402.
5. J. Cea, Approximation variationnelle des problèmes aux limites, Ann. Inst. Fourier, 14 (1964), 345-444.

6. R. Ewing, O. Iliev and R. Lazarov, A modified finite volume approximation of second-order elliptic equations with discontinuous coefficients, *SIAM. J. Sci. Comput.* 23 (2001), 1334-1350.
7. R. D. Lazarov, I. D. Mishev and P. S. Vassilevski, Finite volume methods for convection diffusion problems, *SIAM. J. Num. Anal.* 33 (1996), 31-55.
8. R. E. Ewing, R. D. Lazarov and P. S. Vassilevski, Local refinement techniques for elliptic problems on cell-centred grid, I: Error analysis, *Math. Comp.* 56 (1991), 437-461.
9. A. Tahiri, A compact discretization method for diffusion problems with local mesh refinement, PhD thesis, Service de Métrologie Nucléaire, ULB, Brussels, Belgium, September (2002).
10. A. Tahiri, The PCD method, *Lecture Notes in Computer Science*, 2542 (2003), 563-571.
11. A. Tahiri, Local mesh refinement with the PCD method, *Adv. Dyn. Syst. Appl.* 8(1) (2013), 124-136.
12. A. Tahiri, The PCD Method on Composite Grid, *Bol. Soc. Paran. Mat.* 34(2) (2016), 121-145.
13. A. Tahiri, The best strategy for local mesh refinement with the PCD method, To appear in *International Journal of Dynamical Systems and Differential Equations* (2017).
14. A. Weiser and M. F. Wheeler, On convergence of block-centered finite differences for elliptic problems, *SIAM J. Num. Anal.* 25 (1988), 351-375.

Ahmed Tahiri
Department of Computer Science,
Faculty of Sciences, University Mohammed I,
BP 717 , 60000 Oujda, Morocco .
E-mail address: tahiriahmed02@yahoo.fr